Separation Science and Technology
Publication details, including instructions for authors and subscription information:
http://www.informaworld.com/smpp/title~content=t713708471

TRIANGULAR PHASE DIAGRAMS TO PREDICT THE FRACTIONATION OF FREE FATTY ACID MIXTURES VIA UREA COMPLEX FORMATION

Douglas G. Hayes[a]; James Van Alstine[b]; Anne-Lee Asplund[c]
[a] Department of Chemical and Materials Engineering, University of Alabama in Huntsville, Huntsville, Alabama, U.S.A. [b] Department of Chemistry, University of Alabama in Huntsville, Huntsville, Alabama, U.S.A. [c] Department of Chemical Engineering and Technology, Royal Institute of Technology, Stockholm, Sweden

To cite this Article Hayes, Douglas G. , Van Alstine, James and Asplund, Anne-Lee(2001) 'TRIANGULAR PHASE DIAGRAMS TO PREDICT THE FRACTIONATION OF FREE FATTY ACID MIXTURES VIA UREA COMPLEX FORMATION', Separation Science and Technology, 36: 1, 45 — 58

To link to this Article: DOI: 10.1081/SS-100000850

URL: http://dx.doi.org/10.1081/SS-100000850

SEPARATION SCIENCE AND TECHNOLOGY, 36(1), 45–58 (2001)

TRIANGULAR PHASE DIAGRAMS TO PREDICT THE FRACTIONATION OF FREE FATTY ACID MIXTURES VIA UREA COMPLEX FORMATION

Douglas G. Hayes,[1,*] James Van Alstine,[2,3]
and Anne-Lee Asplund[3]

[1]Department of Chemical and Materials Engineering,
University of Alabama in Huntsville, 130 Engineering
Building, Huntsville, Alabama 35899
[2]Department of Chemistry, University of Alabama in
Huntsville, 203-C Material Sciences Building, Huntsville,
Alabama 35899
[3]Department of Chemical Engineering and Technology,
Royal Institute of Technology, Teknikringen 28, SE-100 44
Stockholm, Sweden

ABSTRACT

The authors previously developed a rapid and inexpensive procedure to fractionate free fatty acid (FFA) mixtures via urea complex (UC) formation. The process yields two phases in equilibrium, a solvent-rich extract phase containing unsaturated FFA and a solid raffinate phase consisting of UCs of saturated and monounsaturated FFA. It effectively removed saturated FFA, that is, palmitic and stearic acid, from an FFA mixture derived from low erucic acid rapeseed (LEAR) oil. In the present study, triangular phase

---

*Address correspondence to D. G. Hayes. E-mail: dhayes@che.uah.edu

www.dekker.com

diagrams were determined for the urea/ethanol/water/LEAR-FFA system at various temperatures, which delineated the phase boundary between the 1-phase and 2-phase regions. Calculations of the amounts and distribution of urea and LEAR-FFA between the two phases based on tie-lines from the phase diagram strongly agreed with experimental data. The diagram accurately predicted the temperature required to cosolubilize urea and LEAR-FFA in solvent. A plot of the percent extraction of an individual FFA species versus percent extraction of total FFA for all major FFA species yielded a universal curve describing results related to various combinations of urea, water, ethanol, and LEAR-FFA. Equations derived from the phase diagram, distribution data for the FFA species, and mass balances were combined to create a mathematical model, which accurately predicted the FFA composition of both phases. The methodology used and results obtained should aid critical evaluation of large scale UC-based FFA fractionation procedures.

Key Words: Extraction; Fatty acid fractionation; Low erucic acid; Rapeseed oil; Urea complex formation.

INTRODUCTION

Innovative methods are needed for the separation of lipids. Currently employed fractionation methods are inadequate for large-scale, cost-effective, environmentally compatible processing. The most common industrial-scale lipid separation technique, molecular distillation, requires high temperatures that may yield undesirable by-products from polyunsaturated fatty acids and has high energy costs (1,2). Other lipid fractionation techniques, such as membrane filtration, winterization, and crystallization, can be slow, inefficient, and expensive. Column chromatography requires significant initial capital outlay and may be better suited to secondary product polishing rather than to primary fractionation.

Fractionation of lipids using urea complex (UC) formation may be a viable primary fractionation method. Urea complexes, first observed in the 1940s (3), consist of spiral, hydrogen-bonded networks of urea molecules surrounding narrow, linear hydrocarbon chains, producing a distinct, stable solid phase. Branched, bulky, double bond-containing, less linearly shaped, and smaller size (e.g., molecular weight) molecules are less likely (energetically favored) to form UCs. The difference in structure of potential guest molecules is the basis of separation. UC-based fractionation is readily scaled up, as it involves low temperatures, simple equipment, and relatively benign reagents (e.g., ethanol, water, and urea), which can often be recycled. As such, UC based processes should have low capital and operating costs and be applicable for preliminary fractionation, particularly in rural settings prior to shipping to an oleochemical processing plant.

The authors recently developed a simple, rapid, robust, adaptable, easily scaled UC-based fractionation procedure. Initial studies demonstrated the effective removal of saturated free fatty acid (FFA) from a low erucic acid rapeseed oil (LEAR) FFA mixture, so as to yield a mono- and polyunsaturated FFA product, which should be of superior nutritional value (4). Preliminary economic analysis suggests the process is competitive, for example, $35 per metric ton processed (5). The UC-based procedure was successfully used to isolate polyunsaturated FFA from fish and borage oil FFA mixtures (6). In addition, various operating parameters have been studied, including the overall mixture and solvent composition, the temperature of UC formation, and the presence of glyceride or phospholipid impurities (4,6).

The UC fractionation process employs three components: urea, LEAR-FFA, and solvent (usually ethanol/water at 95/5 or 90/10, v/v). The solvent, along with slightly elevated temperatures (30–70°C), are required to cosolubilize urea and FFA. Rapid cooling is then applied to lower the system temperature to ambient (ca. 22.5°C), yielding two phases: the solid UC, or "raffinate," phase and the remaining solvent-rich or "extract" phase, containing the FFA product of interest. Because ethanol and water have short chain lengths, they cannot serve as UC templates (3), hence are not incorporated appreciably into the UCs. Each phase was treated with warm (60°C) water to extract away urea and solvent, leaving FFA products behind. On occasion, small amounts of isooctane, a solvent incapable for forming UCs, were included to enhance phase separation. The entire process was operated on the 10- to 100-g scale and occurred within a few minutes (6).

In this report, we present a mathematical model to describe UC fractionation using the urea/ethanol/water/ LEAR-FFA system. The model consists of equations derived from triangular phase diagrams, mass balances, and distribution equations for individual FFA species.

THEORY

The UC fractionation process for the three-component system, urea/solvent/LEAR-FFA, is well described by the principles of liquid–liquid extraction theory (7). Both FFA and urea distribute between the solvent-rich, or extract, phase and the (solid) UC, or raffinate, phase, with the solvent contained almost entirely in the extract phase.

Triangular phase diagrams for the urea/solvent/LEAR-FFA systems employing both 95 and 90% ethanol solvent are depicted in Figure 1 for several equilibrium temperatures. To the right of the phase boundaries exists a single liquid phase region; to the left exists a two-phase region representing liquid (extract) and solid

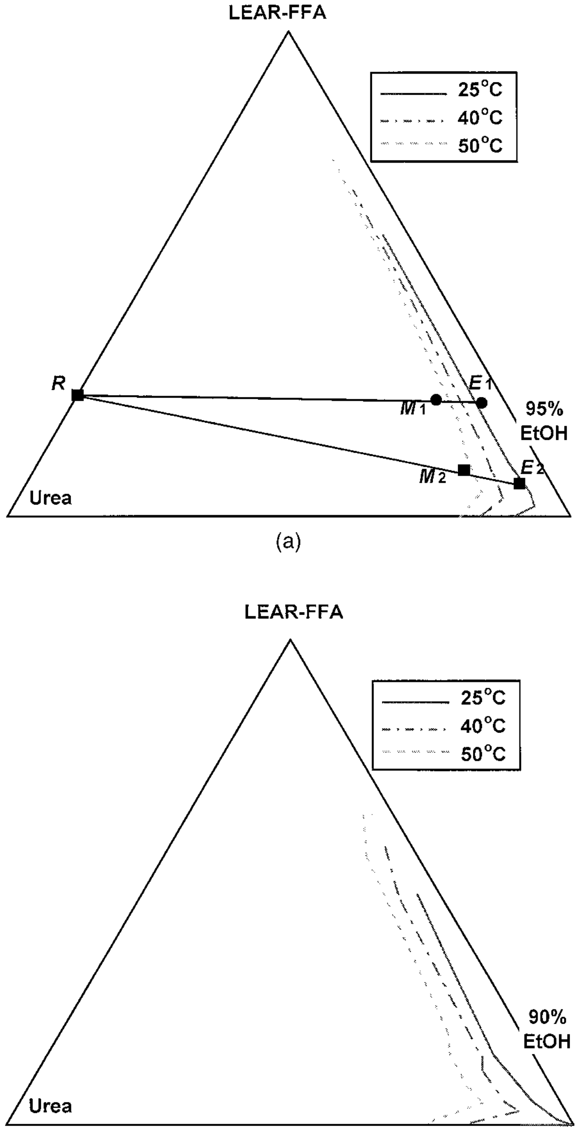

(a)

(b)

Figure 1. Triangular phase diagram, based on mass composition, for the urea/solvent/LEAR-FFA system at 25, 40, and 50°C. a) solvent = 95% ethanol/5% water. b) Solvent = 90% ethanol/10% water. Phase boundaries depict the transition from 2-phase systems (UCs plus liquid phase) to one-phase liquid systems traveling from left to right. Note that LEAR-FFA and 95% ethanol are completely miscible at ambient temperature and above. Lines *E-M1-R1* and *E-M2-R2* are explained in the text.

(UC, or raffinate) in equilibrium. The relative mass of extract and raffinate can be determined from the Lever Rule,

$$R/E = |\text{line } ME|/|\text{line } RM| \tag{1}$$

a line construction on a phase diagram yielding the relative proportions of two phases in equilibrium. Equilibrium tie-lines, required for the Lever Rule, are indicated on Figure 1a. First, the point representing the mixture, M, is located, based on the overall composition by mass of the three components. Point R, representing the raffinate phase, is located in similar fashion, using measured experimental data (4). Because the UCs for LEAR-FFA fractionations contain only urea and FFA at a mole ratio of approximately 13:1 for all cases (4), in agreement with previously reported values for individual FFA species (8,9), point R corresponds approximately to mass fractions of $X_{\text{FFA,R}} = 0.26$, $X_{\text{Urea,R}} = 0.74$, and $X_{\text{EtOH,R}} = 0.00$ for all cases (Fig. 1). Point E, representing the extract phase, then falls at the intersection of line *RM* with the equilibrium curve for the appropriate equilibrium temperature.

Equivalently, a system of four equations, three mass balances [Eqs. (2)–(4)] and an equation to describe the phase boundary [Eq. (5)], are solved simultaneously to yield four unknown variables: the FFA and solvent mass fractions of the extract phase ($X_{\text{FFA,E}}$ and $X_{\text{EtOH,E}}$) and the overall mass of extract and raffinate (E and R, respectively):

$$X_{\text{FFA,M}}M = X_{\text{FFA,R}}R + X_{\text{FFA,E}}E \tag{2}$$

$$X_{\text{EtOH,M}}M = X_{\text{EtOH,E}}E \tag{3}$$

$$M = R + E \tag{4}$$

$$X_{\text{FFA,E}} = \text{function of } (X_{\text{EtOH,E}}, T) \tag{5}$$

The mixture's mass (M) and composition by mass ($X_{\text{FFA,M}}$ and $X_{\text{EtOH,M}}$), as well as the UC formation temperature (T), are predetermined. A more explicit equation for the phase boundary [Eq. (5)] is given below. In addition, Equation (5) can be used to determine the minimum temperature required for cosolubilizing urea, FFA, *and* solvent by substituting $X_{\text{FFA,M}}$ and $X_{\text{EtOH,M}}$ for $X_{\text{FFA,E}}$ and $X_{\text{EtOH,E}}$, respectively, and solving for T.

As discussed below, universal relationships between the precent extraction of FFA species i ($\%Ext_{\text{i}}$) and the percent extraction of total FFA ($\%Ext_{\text{FFA}}$) exist.

$$\%Ext_{\text{i}} = \text{function of } (\%Ext_{\text{FFA}}) \tag{6}$$

This will allow the FFA composition of the extract and raffinate phases to be calculated by using the definitions of $\%Ext_{\text{FFA}}$ and $\%Ext_{\text{i}}$ given in Equations (7) and (8), respectively.

$$\%Ext_{\text{FFA}} = 100\% * X_{\text{FFA,E}}E/X_{\text{FFA,M}}M \tag{7}$$

$$\%Ext_{\text{i}} = Y_{\text{i,E}},\, X_{\text{FFA,E}}E/(Y_{\text{i,M}}X_{\text{FFA,M}}M) = Y_{\text{i,E}}\%Ext_{\text{FFA}}/Y_{\text{i,M}} \tag{8}$$

$Y_{i,E}$ is the fraction of FFA species i among the FFA in the extract. Moreover, Equations (6) to (8) can be solved simultaneously to predict values of $Y_{i,E}$ for each FFA species (i.e., the FFA composition of the *Extract*). Note that $\%Ext_{FFA}$ via Equation (7) is readily calculated, and the composition of LEAR-FFA [$Y_{i,M}$'s, employed in Eq. (8)] is known [$Y_{16:0,M} = 0.046$, $Y_{16:1,M} = 0.002$, $Y_{18:0,M} = 0.020$, $Y_{18:1,M} = 0.603$, $Y_{18:2,M} = 0.243$, $Y_{18:3,M} = 0.069$, $Y_{20:0,M} = 0.006$, $Y_{20:1,M} = 0.013$(4)]. Likewise, the FFA composition of the UCs, or raffinate phase, can be calculated:

$$Y_{i,R} = (100 - \%Ext_i)\, Y_{i,M}/(100 - \%Ext_{FFA}) \qquad (9)$$

A computer program, written using MAPLE mathematical software, employed Equations (2) to (9) to calculate the distribution of FFA and urea between the extract and raffinate, and the composition of FFA species in both phases.

EXPERIMENTAL

LEAR-FFA was a generous donation from Karlshamns, AB (Karlshamn, Sweden). All other materials (ethanol, urea, and deionized water) were of high purity and employed without further purification. Equations (1)–(9) were solved

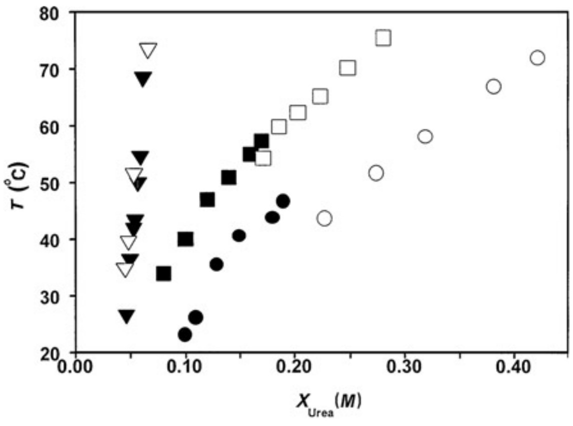

Figure 2. Effect of weight fraction urea in the original mixture, $X_{Urea,M,}$ on the phase boundary temperature, T, for the system urea/solvent/LEAR-FFA. Above the phase transition curve, the system exists as a one-phase liquid; below, UCs are in equilibrium with an ethanolic liquid. Each curve represents the phase transition for specific FFA/urea mass ratio: (circle) 0.0, (square) 1.0, (triangle) 12.0. Filled and unfilled symbols represent 95% ethanol and 90% ethanol as solvent, respectively.

simultaneously using MAPLE V, *Release 5.01 mathematical software (Waterloo Maple, Inc., Waterloo, Ontario).

To determine phase boundaries, a urea/solvent/LEAR-FFA mixture of known composition was heated to obtain homogeneity, then allowed to slowly cool, ultimately yielding a two-phase system. The average temperature at which UC formation was observed indicates the phase boundary (Fig. 2). Typically, a 1–2°C interval existed between the temperature at which small UC crystallites formed and where UC formation was rapid. It was believed that the initial crystallite formation represented local cool spots in the mixture. The temperature at which the crystallites became "numerous," within the temperature interval discussed previously, was used to denote the phase boundary, with error limits of plus/minus 1°C. Several series of experiments were performed, with a given series containing the same FFA/urea mass ratio, but different amounts of solvent.

RESULTS AND DISCUSSION

Phase Diagram and Distribution of LEAR-FFA, Urea, and Solvent

The UC formation temperature was determined experimentally for several series of urea/solvent/LEAR-FFA mixtures using 95 and 90% ethanol (5 and 10% water, respectively) as solvent, where each experiment within a series had the same FFA/urea ratio, but differing amounts of solvent. The phase boundary temperature, T, is plotted versus the mass fraction of urea, $X_{\mathrm{Urea,M,}}$ in Figure 2. At temperatures above the phase boundary, the mixture consisted of a single liquid phase, whereas temperatures below yielded UCs (solid raffinate phase, consisting of FFA and urea) in equilibrium with a solvent-rich liquid (extract) phase. For a given mixture of urea and FFA, the transition temperature decreased in linear fashion as the mixture was diluted with further amounts of solvent (Fig. 2). As the FFA/urea ratio increased, the phase transition shifted to a lower range of $X_{\mathrm{Urea,M}}$, reflecting the lower solubility of urea in the FFA-enriched bulk liquid phase (Fig. 2). Also, the $X_{\mathrm{Urea,M}}$–T phase boundary becomes steeper in slope, indicating a greater sensitivity of phase transition (Fig. 2). Experimental support is found in the phase transition occurring more sharply as the FFA/urea ratio increased. Note that data points for the two solvent systems nearly coincided for a given FFA/urea ratio, which may suggest that the solvent composition does not change the thermodynamics of the UC formation process (Fig. 2). The higher $X_{\mathrm{Urea,M}}$ range for 90% ethanol reflects the greater solubility of urea in this solvent compared to 95% ethanol, whereas the higher T range for this solvent system occurs because of the lower solubility of FFA. The large difference in the shape and position of the phase

---

*The MAPLE V, Release 5.01 program used to predict the outcome of UC-based LEAR-FFA fractionation is readily available from the corresponding author.

boundary in the absence of FFA relative to the presence of FFA is not surprising because in the absence of FFA templates urea forms tetragonal crystals, which are morphologically different from than the hexagonal crystalline UCs (3).

The $X_{\mathrm{Urea,M}}$-T data of Figure 2 was used to produce phase boundaries on urea/solvent/LEAR-FFA triangular phase diagrams at various constant temperatures, 25, 40, and 50°C, for 95 and 90% ethanol (Fig. 1). LEAR-FFA is completely soluble in both solvent systems. As the temperature increases, the 1-phase region increases due to the increased solubility of urea. Note that the boundaries are virtually independent of X_{Urea} for X_{Urea} in the range 0.05–0.10. As X_{FFA} increases, the boundaries at 25, 40, and 50°C nearly coincide, meaning that the influence of temperature is lessened. This mirrors the steepness of the phase boundary curves in Figure 2 for large values of the FFA/urea ratio. The following equations describes the phase boundary for the 95% and 90% ethanol systems [Eqs. (5a) and (5b), respectively] as a function of temperature:

$$\begin{aligned} X_{\mathrm{FFA,E}} &= (-0.905 - 4.42 * 10^{-3}T)X_{\mathrm{EtOH,E}} \\ &\quad + (0.904 + 2.98 * 10^{-3}T - 3.05 * 10^{-5}T^2) \end{aligned} \tag{5a}$$

$$\begin{aligned} X_{\mathrm{FFA,E}} &= (-0.610 - 1.10 * 10^{-2}T)X_{\mathrm{EtOH,E}} \\ &\quad + (0.291 + 3.06 * 10^{-2}T - 3.44 * 10^{-4}T^2) \end{aligned} \tag{5b}$$

When examining the effect of solvent composition, note that the phase boundaries are closer to the urea vertex of the triangular diagram for 90% ethanol, particularly at higher temperatures, reflecting the greater solubility of urea (Fig. 1). These trends, combined with the Lever Rule, indicate that a smaller fraction of raffinate, or UCs, will form for the 90% ethanol system. Phase equilibria experiments were also performed for binary ethanol-water solvent systems containing more than 10% water. Synthesis of a phase diagram was difficult for these systems because of the formation of two liquid phases, due to the low solubility of FFA and the generally low yield of UCs.

The tie-line for a given experiment can be located in Figure 1 by constructing a line through the point representing the composition of the mixture (M) and R, where the location of point R is nearly the same for all tie-lines (discussed above). The composition of the extract phase (point E) is then determined by extending the tie-line to the phase boundary corresponding to the UC formation temperature, T, which usually was room temperature (22.5°C). Data points for two previously published UC-based fractionation experiments (4) are plotted on the triangular phase diagram (Fig. 1a). Their positions are based on experimental measurements. Note that both E_1 and E_2 fall near the phase boundary at 25°C as expected, as the UC formation temperature was about 22.5°C (4). Importantly, data points R, M, and E for each experiment nearly determine a straight line, indicating that the mass balance equations are satisfied. The Lever Rule can therefore be employed to estimate the amount of UCs formed [Eq. (1)].

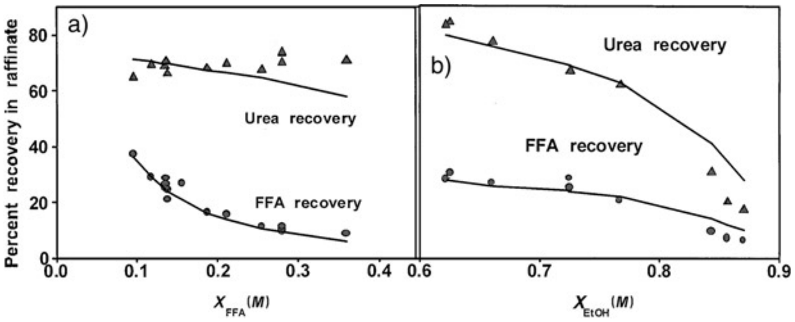

Figure 3. Fit of mathematical model to the recovery of urea and FFA in the UCs (raffinate) to experimental data for the Urea/95% Ethanol/LEAR-FFA system at a UC formation temperature of 22.5°C. Data was taken from Ref. (4). Curves represent predictions by mathematical model. a) Variation of FFA mass, 95% ethanol/urea ratio held at 0.189 g/g; b) variation of 95% ethanol mass, FFA/urea ratio held at 1.00 g/g.

Equations (1) to (5) were solved simultaneously to predict the distribution of three components: urea, LEAR FFA, and solvent. The performance of the model, based on the triangular phase diagram, is demonstrated in Figure 3, where its results are compared with measured experimental values from our previously published data (4). In one case, the FFA amount was varied, holding at the urea/95% ethanol ratio constant (Fig. 3a), and the second case illustrates the effect of the ethanol mass fraction at a constant FFA/urea ratio (Fig. 3b). This figure illustrates the decrease of FFA recovery in the raffinate (UCs) with $X_{\mathrm{FFA,M}}$ and $X_{\mathrm{EtOH,M}}$ because of the limited capacity for FFA in the UC inclusion channels and the partitioning of urea to the solvent, respectively (4). In general, the model performed quite well, with the exception of the urea recovery at high $X_{\mathrm{FFA,M}}$ (Fig. 3a). The difference may be due to the error in assuming that the UC fractionation temperature was exactly 22.5°C, because at high FFA content, the phase boundary is highly sensitive to temperature (Figs. 1 and 2), or that equilibrium had not been reached when the UC formation process was stopped.

Triangular phase diagrams are also useful for predicting the temperature required to cosolubilize urea and LEAR-FFA. For instance, the two series of experiments depicted in Figure 3 require a temperature slightly higher than 50°C for complete miscibility to occur. Predictions from the mathematical model for the effect of FFA and solvent mass fractions on the minimum solubilization temperature for the 95% ethanol solvent system (4) are depicted in Figure 4. The solubilization temperature decreased as the FFA and solvent concentrations were increased, particularly for ethanol, because of the increased urea solubility. A lower solubilization temperature lessens oxidative degradation of unsaturated FFA and the possible formation of toxic carbamate by-products (10). [In the absence of solvent,

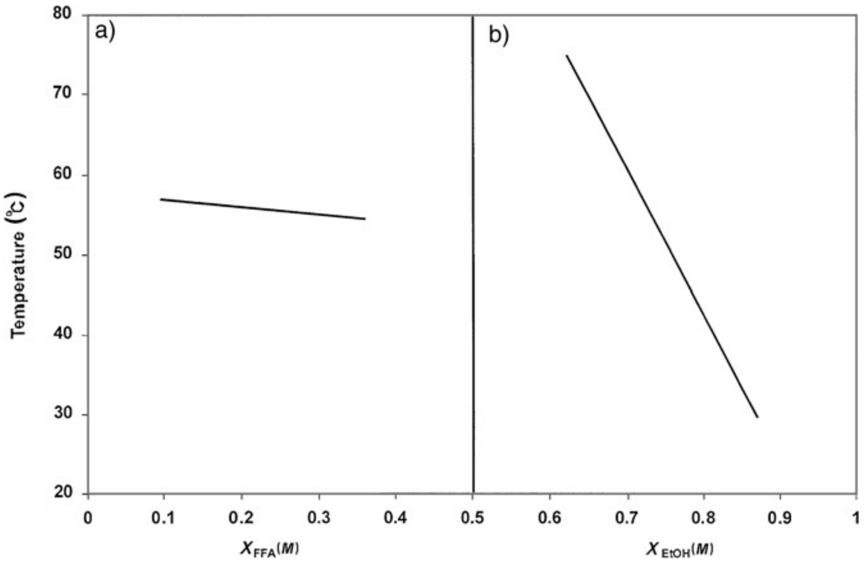

Figure 4. Effect of mixture composition on the solubilization temperature, T, as predicted by the mathematical model. a) Variation of FFA mass, 95% ethanol/urea ratio held at 0.189 g/g; b) variation of 95% ethanol mass, FFA/urea ratio held at 1.00 g/g.

temperatures between 110 and 114°C are required to cosolubilize urea with the FFA species of LEAR (3); and phase diagrams are complex, containing miscibility gaps and a eutectic point (11).]

Distribution of LEAR-FFA Species

An important achievement of the model is the prediction of the FFA composition of the extract and raffinate FFA products. For each FFA species (i), a universal plot of its percent recovery in the extract phase, $\%Ext_{\mathrm{i}}$ [Eq. (8)], versus the percent recovery of LEAR-FFA, [$\%Ext_{\mathrm{FFA}}$, Eq. (7)], using UC-fractionation data from the urea/ethanol/water/LEAR-FFA system and a common UC formation temperature (22.5°C), occurred (Fig. 5). The figure utilizes data from our previous work (4), including the experiments plotted in Figure 3 plus those that applied several different water/ethanol ratios. Other than palmitic acid (16.0), linear models were used to represent the $\%Ext_{\mathrm{FFA}} - \%Ext_{\mathrm{l}}$ relationships for the FFA species (Table 1). The equations' correlation coefficients (R^2 values) for the most abundant species (16:0, 18:1, 18:2, and 18:3) were quite high, whereas the value for 18:0 was lower due to the experimental error in measuring the low 18:0 concentrations

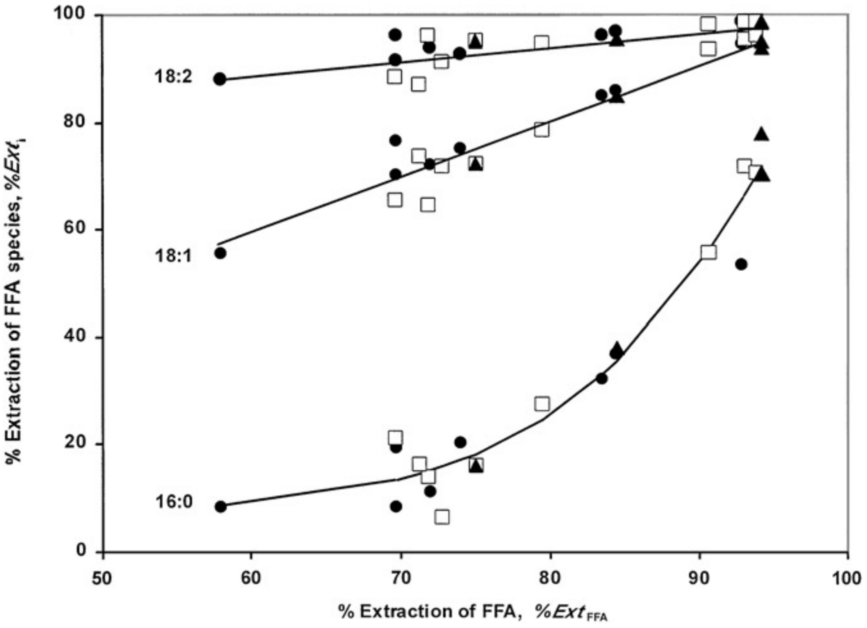

Figure 5. Percent extraction of the individual FFA species as a function of the percent extraction of total FFA for several urea/ethanol/water/LEAR-FFA mixtures. Data was taken from Ref. (4). (Square) Variation of FFA mass, 95% ethanol/urea ratio held at 0.189 g/g; (circle) variation of 95% ethanol mass, FFA/urea ratio held at 1.00 g/g; (triangle) effect of composition of water-ethanol solvent mixture at solvent, FFA, and urea mass fractions of 0.727, 0.137, and 0.137, respectively. Lines and curves represent best least square fits to the data. Equations are listed in Table 1.

Table 1. Equations Relating the Percent Extraction of FFA Species (%Ext_i) Versus the Percent Extraction of FFA (Ext_{FFA}), That is Equation (6)[a]

FFA Species	Equation	R^{2b}
16:0	$\%Ext_{16.0} = -406.5 + 19.21\%Ext_{FFA} - 0.301$ $(\%Ext_{FFA})^2 + 0.00160\ (\%Ext_{FFA})^3$	0.95
18:0	$\%Ext_{18:0} = -69.4 + 1.29\%Ext_{FFA}$	0.66
18:1	$\%Ext_{18:1} = -8.58 + 1.11\%Ext_{FFA}$	0.97
18:2	$\%Ext_{18:2} = 71.1 + 0.30\%Ext_{FFA}$	0.97
18:3	$\%Ext_{18:3} = 82.4 + 0.18\%Ext_{FFA}$	0.83
20.1	$\%Ext_{20:1} = -17.8 + 1.11\%Ext_{FFA}$	0.84

[a] Data is depicted in Figure 5.

[b] Correlation coefficient.

in the extract phase. Equations for two minor components, 20:0 and 16:1, could not be accurately determined. As a first approximation, the 18:1 and 18:0 equations of Table 1 were also employed for 16:1 and 20:0, respectively.

Equations (1)–(5) and (6)–(9) for the most abundant FFA species (i) were solved simultaneously using a Maple V, Release 5.01 worksheet to calculate estimates of the composition of the extract and raffinate FFA mixtures ($Y_{i,E}$ and $Y_{i,R}$, respectively). The model predictions are plotted in Figure 6 against data taken from the experiments represented in Figures 3 and 5. Strong agreement is evident.

Figures 5 and 6 demonstrate important trends useful for applying the UC fractionation process. A low FFA/urea ratio yields an extract product enriched in unsaturated FFA at the cost of reduced recovery (Figs. 3a and 6a). A second

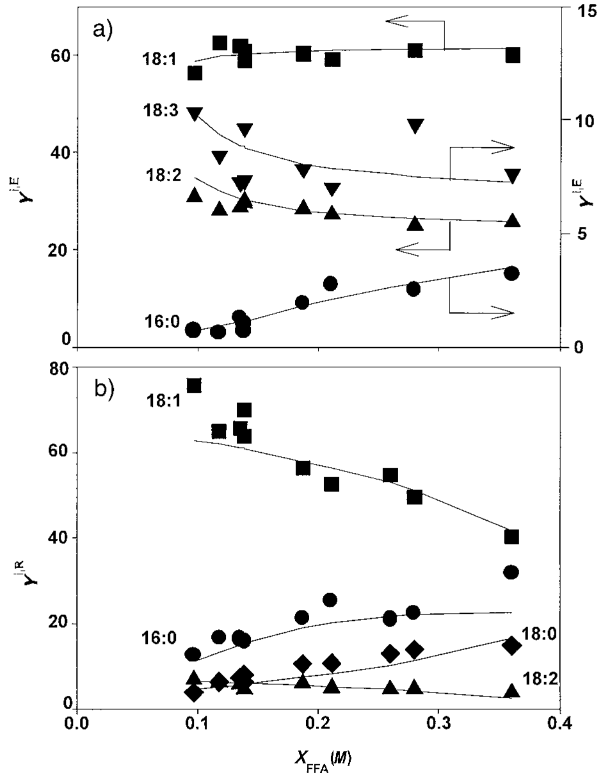

Figure 6. Effect of FFA mass percent in the mixture, $X_{FFA,M}$, on the FFA composition of the a) extract and b) raffinate UC phase. Data taken from Ref. (4). The 95% ethanol/urea ratio held at 0.189 g/g. Curves represent mathematical model prediction. $Y_{i,j}$ refers to the FFA composition of species i in the FFA of phase j.

cost is the reduced oxidative stability of the extract product, due to the increased concentration of 18:2 and 18:3. This suggests a "trade-off effect," indicating that the mixture composition selected will depend on the relative importance of the issues raised above. The distribution data (Fig. 5 and Table 1) demonstrate that FFA species containing shorter chain lengths and greater degrees of unsaturation are enriched in the extract, reflecting the selectivity of UC-based fractionation (6). It is unclear as to the role of the relative concentration of the FFA species on their distribution. Further experimentation, using an FFA mixture containing the same species, but different relative amounts, will assist in this interpretation.

CONCLUSIONS

In summary, the present study involved generation of triangular phase diagrams for various combinations of the four components at various temperatures. These were combined with mass balance equations and distribution data for the FFA species to form a mathematical model that agrees strongly with experimental data and trends. Further experimental and theoretical work is required to adapt this model to alternate solvents and FFA mixtures. However, methodology used and results obtained should aid critical evaluation of large-scale UC-based FFA fractionation procedures.

ACKNOWLEDGMENTS

The authors acknowledge a grant from the Swedish NUTEK Foundation under their New Products from Renewable Resources program, the Swedish NFR, and the U.S. National Aeronautics and Space Administration (NASA). The donation of rapeseed FFA by Karlshamns AB (Karlshamn, Sweden) is gratefully acknowledged.

REFERENCES

1. Shimada, Y.; Sakai, N.; Sugihara, A.; Fujita, H.; Honda, Y.; Tominaga, Y. Large-Scale Purification of γ-Linolenic Acid by Selective Esterification Using Rhizopus Delemar Lipase. J. Am. Oil Chem. Soc. **1998**, *75*, 539–544.
2. Haagsma, N.; van Gent, C.M.; Luten, J.B.; de Jong, R.W.; Van Doorn, E. Preparation of an ω3 Fatty Acid Concentrate from Cod Liver Oil. J. Am. Oil Chem. Soc. **1982**, *59*, 117–118.
3. Swern, D. Urea and Thiourea Complexes in Separating Organic Compounds. Ind. Eng. Chem. **1955**, *47*, 216–221.

4. Hayes, D.G.; Bengtsson, Y.C.; Van Alstine. J.; Setterwall, F. Urea Complexation for the Rapid, Cost Effective, Ecologically Responsible Fractionation of Fatty Acid from Seed Oil. J. Am. Oil Chem. Soc. **1998**, *75*, 1403–1408.
5. Bengtssen, Y.; Hayes, D.G.; Van Alstine, J.M.; Setterwall, F. *Urea Complexation for Separation of Fatty Acids from Seed Oils*, Proceedings of the 89th American Oil Chemists' Society Meeting, Chicago, May 10–13, 1998. Abstract.
6. Hayes D.G.; Van Alstine, J.; Setterwall, F. Urea-Based Fractionation of Fatty Acids and Glycerides of Polyunsaturated and Hydroxy Fatty Acid Seed Oils. J. Am. Oil Chem. Soc. **2000**, *77*, 207–213.
7. Treybal, R.E. *Mass Transfer Operations*, 3rd Ed.; McGraw-Hill: New York; 1980.
8. Knight, H.B.; Witnauer, L.P.; Coleman, J.E.; Noble W.R. Jr.; Swern, D. Dissociation Temperatures of Urea Complexes of Long Chain Fatty Acids, Esters, and Alcohols. Anal. Chem. **1952**, *24*, 331–334.
9. Schlenk, H.; Holman, R.T. Separation and Stabilization of Fatty Acids by Urea Complexes. J. Am. Chem. Soc. **1950**, *72*, 5001–5004.
10. Canas, B.J.; Yurawecz, M.P. Ethyl Carbamate Formation during Urea Complexation for Fractionation of Fatty Acids. J. Am. Oil Chem. Soc. **1999**, *76*, 537.
11. Kuhnert-Brandstatter, M.; Burger, A. Phase Diagrams of Urea Inclusion Compounds. Part 1: Palmitic Acid and Urea. Pharmazie. **1996**, *51*, 288–292.

Received February 2, 2000
Revised April 2000

Downloaded At: 10:52 25 January 2011

Request Permission or Order Reprints Instantly!

Interested in copying and sharing this article? In most cases, U.S. Copyright Law requires that you get permission from the article's rightsholder before using copyrighted content.

All information and materials found in this article, including but not limited to text, trademarks, patents, logos, graphics and images (the "Materials"), are the copyrighted works and other forms of intellectual property of Marcel Dekker, Inc., or its licensors. All rights not expressly granted are reserved.

Get permission to lawfully reproduce and distribute the Materials or order reprints quickly and painlessly. Simply click on the "Request Permission/Reprints Here" link below and follow the instructions. Visit the U.S. Copyright Office for information on Fair Use limitations of U.S. copyright law. Please refer to The Association of American Publishers' (AAP) website for guidelines on Fair Use in the Classroom.

The Materials are for your personal use only and cannot be reformatted, reposted, resold or distributed by electronic means or otherwise without permission from Marcel Dekker, Inc. Marcel Dekker, Inc. grants you the limited right to display the Materials only on your personal computer or personal wireless device, and to copy and download single copies of such Materials provided that any copyright, trademark or other notice appearing on such Materials is also retained by, displayed, copied or downloaded as part of the Materials and is not removed or obscured, and provided you do not edit, modify, alter or enhance the Materials. Please refer to our Website User Agreement for more details.

Order now!

Reprints of this article can also be ordered at
http://www.dekker.com/servlet/product/DOI/101081SS100000850